the incident neutron beam in the graphite. The interesting feature of Fig. 4 is the significant rise in scattered intensity at the point A, which is well resolved from the pseudo-elastic peak. It seems reasonable to identify the increased scattered intensity as being associated with low-frequency transverse modes propagated along or nearly along the [001] axis, and to assign them frequencies of the order of 1.0×10^{12} cps. Other, similar experiments which we have performed support this explanation, but do not fully confirm it.

Assuming our interpretation is correct, then a consideration of the data obtained leads to a frequency at the zone boundary of $(1.3\pm0.3)\times10^{12}$ cps for the transverse mode with wave vector parallel to the [001] axis. On the further assumption that the dispersion curve is a simple sine curve, as in the L[001] case, we can deduce a rough value for the elastic constant C_{44}. This is listed in Table I together with previous estimates of this quantity.

DISCUSSION

In the previous section measurements were presented of those vibrations of the graphite lattice in which undistorted hexagonal planes of carbon atoms moved relative to each other in two distinct modes, longitudinal and transverse. The dispersion relation for the longitudinal, L[001], modes (involving variation of the interplanar spacing) has been completely and unambiguously measured. The dispersion curve is very well fitted by a two-term Fourier series of the form[18,19]

$$4\pi^2M\nu^2=A_1(1-\cos\tfrac{1}{2}cq)+A_2(1-\cos cq), \qquad (2)$$

where M is the mass of the carbon atom, and the coefficient (or force constant) A_2 is 1.6% of A_1. Additional Fourier terms do not significantly improve the fit to the experimental results. The least-squares Fourier analysis was performed using the Datatron computer. The solid line in Fig. 3 is the best fit to the results if only one Fourier component is employed. In this L[001] mode of vibration, the individual sheets of carbon atoms remain undistorted while the interplanar distance is varying. The forces involved are thus purely interplanar, and the excellent fit displayed in Fig. 3, indicates that these interplanar forces are almost entirely between nearest-neighbor planes.

The observation of the transverse modes (involving sliding motions of the plans of atoms) is necessarily more tentative, but we feel the interpretation given in the previous section is probably correct. The first-neighbor interplanar force constant relating to these transverse modes is about 10% of the analogous L[001] force constant. This is substantially higher than would be expected on the basis of a model of the graphite lattice involving simple r^{-n} short-range repulsive, and Van der Waals r^{-6} attractive, interatomic forces.

ACKNOWLEDGMENTS

We are very grateful to Dr. R. J. Diefendorf and the General Electric Company (Schenectady, N. Y.) for providing the excellent specimen which made these experiments possible. We also thank Professor J. Krumhansl for his good offices in obtaining the specimen.

[18] A. J. E. Foreman and W. M. Lomer, Proc. Phys. Soc. (London) **B70**, 1143 (1957).
[19] B. N. Brockhouse, T. Arase, G. Caglioti, K. R. Rao, and A. D. B. Woods, Phys. Rev. **128**, 1099 (1962).

PHYSICAL REVIEW VOLUME 128, NUMBER 3 NOVEMBER 1, 1962

Escape Mechanism of Secondary Electrons in Polar Crystals*

W. S. KHOKLEY AND K. M. VAN VLIET
Department of Electrical Engineering, University of Minnesota, Minneapolis, Minnesota
(Received March 26, 1962)

A simplified theory for the motion of secondary electrons produced inside a solid by electron bombardment is proposed. The Boltzmann transport equation is solved for scattering due to electron-phonon collisions. Forward scattering is found to be very predominant, and accordingly the scattering integral is greatly simplified if, further, a constant energy loss per collision can be assumed. Postulating also a form for the internal excitation function, the solution is obtained and applied to calculate the energy distribution, the angular dependence, and the dependence of the total external current on the electron affinity. Despite the oversimplified assumptions the model clearly shows the difference with the theories given for metals by Wolff and others. Several experimental features as observed on MgO are compatible with the theory.

1. INTRODUCTION

IN the theory of secondary emission of electrons from a solid usually two steps are distinguished. The first one is concerned with the production of secondary electrons inside the material resulting from the bombardment by the primary electron source. Basically a computation of this nature requires a knowledge of the electron wave functions in the solid, its band structure, and the matrix elements for the interacting potential. Such theories have been given by several authors and have been summarized in papers by Dekker and van

* This research was supported by the United States Air Force, AFSC, Aeronautical Systems Division, Contract Nos. 33(616)-6239 and 33(657)-8040.

der Ziel[1] and Streitwolf.[2] The second phase in the calculation of the secondary emission coefficient δ—which is defined as the ratio of the secondaries emerging from the solid to the number of primaries incident on the crystal—involves the consideration of the transport of internally created secondaries to the surface of the sample. In the most simple phenomenological theories a mere exponential or Gaussian escape function is employed to that effect, utilizing an effective escape depth that may range from 20Å in metals to about 1000 Å in insulators. Obviously, the transport processes in both classes of materials are quite different; in metals the main source of scattering and slowing down of the internal electrons is caused by electron-electron scattering, whereas in insulators scattering with lattice vibrations prevails. A theory of the escape in metals has been given before by Wolff[3] based on the slowing-down equation well known in neutron physics as formulated by Marshak and others.[4] An extension of this work is to be found in a survey paper by Hachenberg and Brauer.[5] An attempt at a theory for insulators will be given here, based on the Boltzmann transport equation. However, greatly simplifying assumptions will be made in order to arrive at some general conclusions concerning the energy distribution, angular dependence, and work-function dependence for the secondary emission from insulators—like MgO and alkali halides—and in order to stress the difference with scattering processes in metals. In the present paper it will be assumed that the electrons move in the absence of external force fields. In a forthcoming paper the effect of an electric field on the motion of the secondaries to the surface and the enhancement or dehancement of the secondary-yield coefficient δ caused by such a field will be investigated.

The assumptions made in the present article can be summarized as follows:

(1) The incidence of the primary-electron beam is such that the spatial dependence of the internal secondary-electron distribution is one-dimensional.

(2) The secondary electrons move in a simple conduction band where the energy is measured relative to the bottom of the conduction band, i.e., $\epsilon=\hbar^2k^2/2m^*$, where m^* is the isotropic effective mass.

(3) The electrons interact only with the lattice vibrations. For ionic crystals the further simplification can be made that only the optical polar modes are of interest, to which modes we assign the same frequency $\omega_{\mathbf{q}}$, $\mathbf{q}$ ranging in the first Brillouin zone.

(4) The mean free path λ depends only on $|k|$ and not on the direction of motion.

2. THE TRANSPORT EQUATION

Let $f(\mathbf{r},\mathbf{k})d\mathbf{r}d\mathbf{k}$ be the probability of finding the electron at position between $\mathbf{r}$ and $\mathbf{r}+d\mathbf{r}$ with crystal momentum between $\mathbf{k}$ and $\mathbf{k}+d\mathbf{k}$. The equation governing $f(\mathbf{r},\mathbf{k})$ in the presence of scattering and in the presence of external forces is

$$\mathbf{v}\cdot\mathrm{grad}_{\mathbf{r}}f(\mathbf{r},\mathbf{k})+\hbar^{-1}\mathbf{F}\cdot\mathrm{grad}_{\mathbf{k}}f(\mathbf{r},\mathbf{k})$$
$$=\int f(\mathbf{r},\mathbf{k}')[1-f(\mathbf{r},\mathbf{k})]P(\mathbf{k}'\rightarrow\mathbf{k})d\mathbf{k}'$$
$$-\int f(\mathbf{r},\mathbf{k})[1-f(\mathbf{r},\mathbf{k}')]P(\mathbf{k}\rightarrow\mathbf{k}')d\mathbf{k}'+S(\mathbf{r},\mathbf{k}). \quad (1)$$

Here $\mathbf{v}$ is the velocity of the particle, $\mathbf{F}$ is the force on the particle, $P(\mathbf{k}'\rightarrow\mathbf{k})$ is the probability per unit time that an electron goes from an occupied state $\mathbf{k}'$ to an unoccupied state $\mathbf{k}$ and similarly for $P(\mathbf{k}\rightarrow\mathbf{k}')$; $S(\mathbf{r},\mathbf{k})$ is the source of the electrons. Further, at more remote points there will be a drain of electrons to make the distribution stationary. We shall assume that there is a large number of vacant states in the conduction band. So $1-f(\mathbf{r},\mathbf{k})$ can be approximated to 1. Further, let

$$\int f(\mathbf{r},\mathbf{k})P(\mathbf{k}\rightarrow\mathbf{k}')d\mathbf{k}'=f(\mathbf{r},\mathbf{k})v(\mathbf{k})/\lambda(\mathbf{k}) \quad (2)$$

define a mean free path $\lambda(\mathbf{k})$. Also, the second integral in the collision term will be modified by changing the transition rate per unit time to the probability per scattering process

$$P(\mathbf{k}'\rightarrow\mathbf{k})=Q(\mathbf{k}'\rightarrow\mathbf{k})v(\mathbf{k}')/\lambda(\mathbf{k}'), \quad (3)$$

where $Q(\mathbf{k}'\rightarrow\mathbf{k})$ is proportional to the differential cross section. Further, as usual, the variable $\mathbf{k}$ will be represented by ϵ and $\boldsymbol{\Omega}$, where $\boldsymbol{\Omega}$ is a unit vector in the scattering direction. Then the Boltzmann equation becomes

$$\mathbf{v}\cdot\mathrm{grad}F(\mathbf{r},\epsilon,\boldsymbol{\Omega})+\frac{v(\epsilon)}{\lambda(\epsilon)}F(\mathbf{r},\epsilon,\boldsymbol{\Omega})$$
$$=\int\int F(\mathbf{r},\epsilon,\boldsymbol{\Omega}')Q(\epsilon',\boldsymbol{\Omega}'\rightarrow\epsilon,\boldsymbol{\Omega})\frac{v(\epsilon')}{\lambda(\epsilon')}d\epsilon'd\boldsymbol{\Omega}'$$
$$+S(\mathbf{r},\epsilon,\boldsymbol{\Omega}), \quad (4)$$

where $F=f(2\epsilon)^{\frac{1}{2}}(m/\hbar^2)^{\frac{3}{2}}$ refers to the distribution per unit energy interval per unit solid angle.

The scattering function Q can be obtained from the theory of optical phonon scattering, as, e.g., given by Dekker.[6] For most of the energy range of interest

[1] A. J. Dekker and A. van der Ziel, Phys. Rev. **86**, 755 (1952).
[2] M. W. Streitwolf, Ann. Physik **3**, 183 (1959).
[3] P. A. Wolff, Phys. Rev. **95**, 56 (1954).
[4] R. E. Marshak, Revs. Modern Phys. **19**, 185 (1947).
[5] O. Hachenberg and W. Brauer, in *Advances in Electronics and Electron Physics*, edited by L. Marton (Academic Press Inc., New York, 1959), Vol. 11.
[6] A. J. Dekker, Second Quarterly Report Secondary Emission Project No. DA 36-039 sc-42561, June 1, 1953 to Sept. 1, 1953 (unpublished), p. 35. See also J. M. Ziman, *Electrons and Phonons* (Oxford University Press, New York, 1960), Chap. 5.

(except for very low energies) one finds that Q can be split into an angular dependent part $Q_1(\Omega' \rightarrow \Omega)$ and an energy dependent part $Q_2(\epsilon' \rightarrow \epsilon)$; the angular part is proportional to $(\sin\frac{1}{2}\beta)^{-2}$, where $\beta=\cos^{-1}(\Omega'\cdot\Omega)$. Let ϕ and θ represent the polar angles for Ω, with the x direction chosen normal to the surface as polar axis, (see Fig. 1) and let $\mu=\cos\theta$, then from simple geometry:

$$\cos\beta=\mu\mu'+(1-\mu^2)^{\frac{1}{2}}(1-\mu'^2)^{\frac{1}{2}}\cos(\phi-\phi'). \quad (5)$$

Since we have a plane source, F will be independent of ϕ. Hence the integration in (4) over ϕ can be carried out yielding

$$Q_1(\Omega' \rightarrow \Omega)d\phi \propto \int_0^{2\pi} (\sin\tfrac{1}{2}\beta)^{-2}d\phi=\frac{4\pi}{|\mu-\mu'|}. \quad (6)$$

This result strictly does not hold for $\mu=\mu'$, since the approximate form $(\sin\frac{1}{2}\beta)^{-2}$ for the scattering function does not hold for extremely small scattering angles. From (6) it can be expected, however, that for $\mu \rightarrow \mu'$, Q_1 has a strong maximum, though the integral of Q_1 over $d\Omega'$ should remain finite [and equal to 1, according to (2) and (3)]. In order to continue the problem rigorously, we should employ more details about the scattering function; the use of (6) will lead to an integro-partial-differential equation, which with suitable transform methods can be reduced to a Fredholm-type integral equation, the Kernel of which shows a singularity for $\mu=\mu'$. Though this problem is being further investigated, in the present paper we shall drastically simplify the solution by replacing the approximate scattering function (6) by $\delta(\mu-\mu')$, indicating strongly forward scattering. This way we shall be led to a simple analytical solution. Even though the percentage error due to this approximation cannot be estimated until the problem is solved more rigorously, it should be noted that this theory will clearly reveal the difference with the behavior in metals, for which the scattering function is usually approximated by the other extreme possibility of nearly spherically symmetric scattering (compare Wolff[3]).

Further, it is shown in the paper on electron-phonon scattering[6] that, on the average, energy is lost per collision, i.e., phonon emissive processes are much more abundant than phonon absorptive processes, such that the average loss per collision is given by

$$a(\epsilon)=\hbar\omega_q \tanh(\hbar\omega_q/2kT). \quad (7)$$

This expression for $a(\epsilon)$ is particularly simple for optical phonon scattering in ionic crystals in the sense that it is independent of the electron energy ϵ. This approximation is justified for electrons, say, above 1 eV, as $a(\epsilon)$ is about 0.1 eV for MgO at room temperature and decreases to 0.06 eV at 740°C. Again, since the complete expression for the energy loss distribution is quite involved we shall approximate by

$$Q_2(\epsilon' \rightarrow \epsilon)=\delta[\epsilon'-\epsilon-a(\epsilon)]. \quad (8)$$

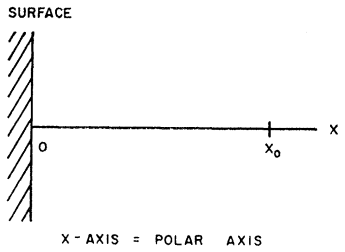

FIG. 1. Geometry employed in model. At $x=0$, there is a surface, and at x_0 there is a plane source.

With these functions for Q_1 and Q_2, the Eq. (4) results in

$$v(\epsilon)\mu\frac{\partial F(x,\epsilon,\mu)}{\partial x}+\frac{v(\epsilon)}{\lambda(\epsilon)}F(x,\epsilon,\mu)=\frac{v(\epsilon+a)}{\lambda(\epsilon+a)}F(x,\epsilon+a,\mu)+S(x,\epsilon,\mu). \quad (9)$$

We can think of the energy-loss process as a continuous one. Since $a \ll \epsilon$ for the range of energies of interest, we can use the following approximation to Eq. (9):

$$v(\epsilon)\mu\frac{\partial F(x,\epsilon,\mu)}{\partial x}=a\frac{\partial}{\partial\epsilon}\left(\frac{v(\epsilon)}{\lambda(\epsilon)}F(x,\epsilon,\mu)\right)+S(x,\epsilon,\mu).$$

Putting

$$\frac{v(\epsilon)}{\lambda(\epsilon)}F(x,\epsilon,\mu)=\psi(x,\epsilon,\mu),$$

we finally get

$$\lambda(\epsilon)\mu\frac{\partial\psi}{\partial x}(x,\epsilon,\mu)-a\frac{\partial\psi}{\partial\epsilon}(x,\epsilon,\mu)=S(x,\epsilon,\mu). \quad (10)$$

This equation can be further simplified by introducing the new variable

$$\eta=\int_0^{\epsilon}\lambda(\epsilon')d\epsilon'.$$

Putting also for the source

$$S(x,\eta,\mu)/\lambda(\eta)=\sigma(x,\eta,\mu),$$

we obtain

$$\mu\frac{\partial\psi}{\partial x}(x,\eta,\mu)-a\frac{\partial\psi}{\partial\eta}(x,\eta,\mu)=\sigma(x,\eta,\mu). \quad (11)$$

3. SOLUTION OF THE TRANSPORT EQUATION

A general solution of Eq. (11) is easily obtained providing $\sigma(x,\eta,\mu)$ behaves suitably at $x=\pm\infty$. In the Appendix the solution is shown to be

$$\psi(x,\eta,\mu)=\frac{1}{a}\int_{\eta}^{\eta_0}d\eta'\,\sigma\left[x+\frac{\mu}{a}(\eta-\eta'),\eta',\mu\right]. \quad (12)$$

Dekker[6] has shown that for the energy range con-

cerned with, $\lambda(\epsilon)$ may be approximated as

$$\lambda(\epsilon)=c\epsilon^{\alpha}, \tag{13}$$

where α is a positive number ranging between 0.5 and 1.0. More exact expressions have also been given by Fröhlich.[7] From Eq. (12) then

$$\psi(x,\epsilon,\mu)=\frac{1}{a}\int_{[c/(\alpha+1)]\epsilon^{\alpha+1}}^{[c/(\alpha+1)]\epsilon_0^{\alpha+1}} d\epsilon' S\left[x+\frac{\mu c}{a(\alpha+1)}\times(\epsilon^{\alpha+1}-\epsilon'^{\alpha+1}),\ \epsilon',\ \mu\right]. \tag{14}$$

To discuss the solution, the source function $S(x,\epsilon,\mu)$ must be known. Various approximating theories have been given for the production of secondaries in metals,[1,2,5] but little work has been done with respect to insulators. In order to determine the spatial distribution of the produced secondaries, it has been assumed in most theories that the production is proportional to the energy dissipation. Recent experiments by Arntz and van Vliet[8] indicate that this may not be the case. Thus, several semiempirical theories are not applicable. Experimentally, information on the production function is available in papers by Young on the transmission of electrons in Al_2O_3,[9] and from coloration in KCl single crystals after bombarding with electrons.[5] The interpretation of these data is not unambiguous. Often, Young's data have been interpreted in terms of a uniform excitation of secondaries over a depth d from the surface (so-called "constant-loss" theory, compare Dekker)[10]; a recent reinterpretation of these data by Arntz indicates a maximum occurring near the end of the primary track, especially for higher primary energies. Lacking detailed information, we shall presently restrict ourselves to an extreme model in which production of secondaries occurs at $x=x_0$ only. It will be assumed that the depth x_0 is of the order of the range d of the primaries. Next, in deciding on the energy dependence of the source, we shall take a general power law $S\propto\epsilon^{-n}$, where n is a small positive number. Under very simplifying assumptions, an exact square law is found[5] (i.e., $n=2$):

$$S(\epsilon)=\frac{e^4N^3|F|^2G}{16\pi\kappa E_p\epsilon^2},\quad \epsilon\geq\frac{(\Delta E_g)^2}{4E_p}, \tag{15}$$

where N is the number of ion pairs per unit volume, G is the valency, κ is the dielectric constant, E_p is the primary energy, ΔE_g is the bandgap, and F is a "form factor," involving the Bloch wave functions of the material. The angular dependence of secondaries produced in insulators is another point that needs more investigation.

In view of these remarks, we shall represent the source function in this paper by

$$S(x,\epsilon,\mu)=A\delta(x-x_0)\epsilon^{-n}g(\mu).$$

Some more specific restrictions will be made later.

Due to the scattering processes assumed we expect symmetry of the solution about $x=x_0$. The Eq. (11) shows that $(x-x_0)/\mu$ is always positive as $1>\mu>0$ for $x>x_0$ and $-1<\mu<0$ for $x<x_0$. For this case the solution becomes

$$\psi(x,\epsilon,\mu)=\frac{Ag(\mu)}{\mu c}\left(\frac{c}{\alpha+1}\right)^{(n+\alpha)/(\alpha+1)}\times\left[\frac{(x-x_0)a}{\mu}+\frac{c}{\alpha+1}\epsilon^{\alpha+1}\right]^{-(n+\alpha)/(\alpha+1)}, \tag{16}$$

where ϵ_0 has been chosen infinity indicating that no electrons of infinite energy occur. More strictly, one should impose a maximum energy ϵ_0 at the source. The maximum energy at any point x, $\epsilon_0(x)$ is then found to be a decreasing function of $x-x_0$ due to slowing down by the scattering.

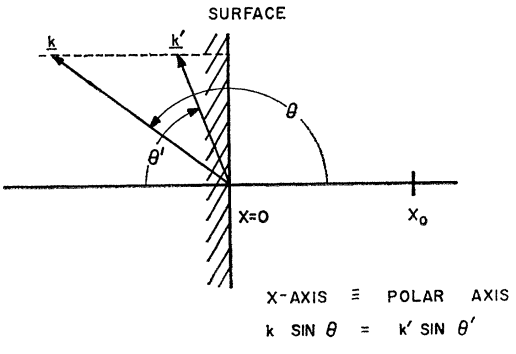

FIG. 2. The effect of the surface potential barrier on the crystal momentum.

4. ESCAPE MECHANISM

We consider a semi-infinite slab of material lying to the right of the $x=0$ plane (Fig. 2). A potential barrier of ωeV exists at the boundary at $x=0$. For $\frac{1}{2}mv_x^2\geq\omega$ most electrons will escape; we shall neglect the few electrons which are reflected back into the material for $\frac{1}{2}mv_x^2\geq\omega$. For smaller energies there is a marked effect on the internal energy distribution but since these electrons do not escape we are not interested in this group. The current density coming out of the material within the range $d\epsilon d\mu$ (of internal energy and angle parameters) is

$$j(\epsilon,\mu)d\epsilon d\mu=v\mu F(0,\epsilon,\mu)d\epsilon d\mu=\mu\lambda(\epsilon)\psi(0,\epsilon,\mu)d\epsilon d\mu. \tag{17}$$

[7] H. Fröhlich, Proc. Roy. Soc. (London) **160**, 230 (1937); **172**, 94 (1939)
[8] F. O. Arntz and K. M. van Vliet, J. Appl. Phys. **33**, 1563 (1961).
[9] J. R Young, Phys. Rev. **103**, 292 (1956).
[10] A. J. Dekker, in *Solid-State Physics*, edited by F. Seitz and D. Turnbull (Academic Press Inc., New York, 1958), Vol. 6.

Here ϵ and μ are now bounded by the following region:

$$\tfrac{1}{2}mv_x^2 \geq \omega,$$

or

$$\epsilon_0(0) \equiv \epsilon_{00} \geq \epsilon \geq \omega/\mu^2,$$
$$(\omega/\epsilon_{00})^{\frac{1}{2}} \leq \mu \leq 1. \tag{18}$$

The total current is given by

$$j_{\text{total}} = \int_{(\omega/\epsilon_{00})^{1/2}}^{1} d\mu \int_{\omega/\mu^2}^{\epsilon_{00}} d\epsilon\, j(\epsilon,\mu)$$
$$= \int_{\omega}^{\epsilon_{00}} d\epsilon \int_{(\omega/\epsilon)^{1/2}}^{1} d\mu\, j(\epsilon,\mu). \tag{19}$$

Hence the energy distribution is found as

$$j(\epsilon) = \int_{(\omega/\epsilon)^{1/2}}^{1} j(\epsilon,\mu)d\mu, \tag{20}$$

which can easily be converted to the external energy distribution, replacing ϵ by $\epsilon = \epsilon' + \omega$. The angular distribution is found to be

$$j(\mu) = \int_{\omega/\mu^2}^{\epsilon_{00}} j(\epsilon,\mu)d\epsilon. \tag{21}$$

However, only for very low ω, this result will resemble the externally measured angular distribution. More generally, one has to proceed as follows: Momentum and energy conservation lead to

$$\epsilon = \epsilon' + \omega \quad \text{or} \quad \hbar^2k^2 = \hbar^2k'^2 + 2m\omega,$$
$$k\sin\theta = k'\sin\theta', \tag{22}$$

where θ' is the external polar angle. Inversion of Eq. (22) yields

$$\epsilon = \epsilon' + \omega,$$
$$\mu = \left[\frac{\omega}{\epsilon'+\omega} + \frac{\epsilon'}{\epsilon'+\omega}\cos^2\theta'\right]^{\frac{1}{2}}. \tag{23}$$

Further, since the Jacobian is

$$\frac{\partial(\epsilon,\mu)}{\partial(\epsilon',\cos\theta')} = \frac{\cos\theta'}{\mu}\frac{\epsilon'}{\epsilon'+\omega}, \tag{24}$$

the distribution in terms of the external parameters ϵ' and $\cos\theta'$ becomes

$$j(\epsilon',\cos\theta')d\epsilon' d(\cos\theta')$$
$$= \lambda(\epsilon'+\omega)\psi[0,\ \epsilon'+\omega,\ \mu(\epsilon',\cos\theta')]\frac{\epsilon'}{\epsilon'+\omega}$$
$$\times\cos\theta' d\epsilon' d(\cos\theta'). \tag{25}$$

The distribution $j(\cos\theta')$ is found by integrating over all ϵ' from zero to infinity after substituting for $\mu(\epsilon',\cos\theta')$ from Eq. (23). Equation (25) also gives directly the energy angular distribution $j(\epsilon',\cos\theta')$.

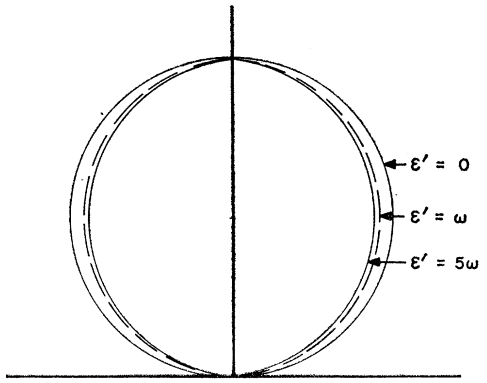

FIG. 3. Energy angular distribution of outcoming secondaries for various ϵ'/ω.

5. EXAMPLE

We apply the above theory to an ionic crystal, for example, MgO. From reference (6), we obtain $\lambda(\epsilon) = 1.6\epsilon$ Å, where ϵ is in eV for a range from 1 to 10 eV.

The exponent in the excitation function ϵ^{-n} will be taken as $n=2$. For $g(\mu)$ we shall tentatively take an isotropic distribution, i.e., $g(\mu)=1$. The constant A of the internal source function depends on the primary energy, (see below).

Hence, for this case Eq. (15) yields

$$\psi(0,\epsilon,\mu) = \frac{A}{|\mu|c}\left(\frac{c}{2}\right)^{\frac{3}{2}}\left[\frac{da}{\mu} + \frac{c}{2}\epsilon^2\right]^{-\frac{3}{2}}, \tag{26}$$

where d is the distance of the source from the surface, which roughly may be identified with the range of the primary electrons (provided most secondaries are produced at the end of the range for which there is ample evidence in production theories); hence it is of the order of 500 Å for 1-keV electrons in MgO. The average energy loss is about 0.1 eV for internal secondaries of energies above 1 eV.

A. Energy Angular Dependence

We find from Eq. (26) for $\epsilon \ll (2da/c)^{\frac{1}{3}} \sim 7$ eV, ψ is proportional to $\mu^{\frac{3}{2}}$. Converting to the $\cos\theta'$ distribution we obtain [Eq. (25)]:

$$\frac{j(\epsilon',\cos\theta')}{j(\epsilon',1)} = \left[\frac{\omega}{\epsilon'+\omega} + \frac{\epsilon'}{\epsilon'+\omega}\cos^2\theta'\right]^{\frac{1}{2}}\cos\theta'. \tag{27}$$

The results are plotted in Fig. 3.

For extremely low ϵ', this is a $\cos\theta'$ distribution as is also observed experimentally by Jonker[11] and calculated

[11] J. L. H. Jonker, Philips Research Repts. 12, 249(1957.)

theoretically by Stolz[12] for metals. For insulators on measurements have been reported to the knowledge of the authors.

B. Angular Dependence

The integral (21) is found to be

$$j(\mu)=\frac{2A}{c}\left(\frac{c}{2}\right)^{\frac{3}{2}}\left[\left(\frac{\mu^4}{da\mu^3+c\omega^2/2}\right)^{\frac{1}{2}}-\left(\frac{\mu}{c\epsilon_{00}^2\mu/2+da}\right)^{\frac{1}{2}}\right]. \quad (28)$$

The result is plotted in Fig. 4 where we took $d=300$ Å, $a=0.1$ eV, $c=1.6$, $\omega=0.5$, and 1.0 eV; the choice of ϵ_{00} is somewhat arbitrary. For $\epsilon_{00}=10$ eV (corresponding to a cutoff of about 15 eV at the source), the dependence as shown in the figure resembles a linear μ relationship. A higher ϵ_{00} makes the curves more convex.

Figure 4 indicates further that the electrons escape only when their direction cosine μ is more than a certain value, being $(\omega/\epsilon_{00})^{\frac{1}{2}}$. E.g., for $\omega=0.5$ eV and $\epsilon_{00}=10$ eV, this "escape cone" has an apex angle of 77°. Electrons coming out in directions with $\theta>77°$ cannot escape.

As stated earlier, the dependence of j on $\mu=\cos\theta$ will be similar to the dependence of the external angle $\cos\theta'$ if ω is small. This was verified by integrating Eq. (25) over $d\epsilon'$, employing an ERA 1103 computer. The results are shown in Fig. 5. For $\epsilon_{00}=10$ eV, the variation of j with $\cos\theta'$ is even closer to linear than before. If $\epsilon_{00}\rightarrow\infty$, the curves become again convex.

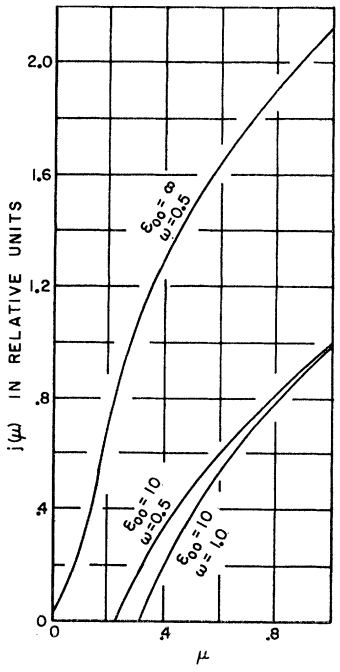

FIG. 4. Angular distribution of internal secondaries at the surface normalized to unity for $\mu=1$, $\omega=0.5$ eV and $\epsilon_{00}=10$ eV.

[12] M. Stolz, Ann. Physik 3, 197 (1959).

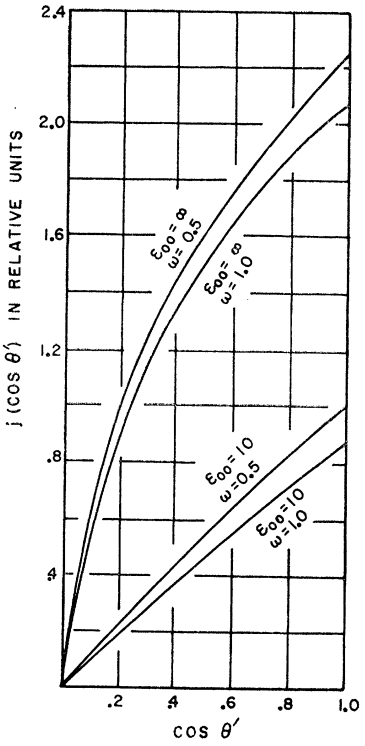

FIG. 5. Angular distribution of external secondaries normalized to unity for $\cos\theta'=1$, $\omega=0.5$ eV and $\epsilon_{00}=10$ eV.

C. Energy Distribution

From Eq. (20) we obtain with $\alpha=1$:

$$j(\epsilon')=\frac{A}{(\epsilon'+\omega)^2}\left\{\left[1+\frac{2ad}{c(\epsilon'+\omega)^2}\right]^{-\frac{1}{2}}-\left(\frac{\omega}{\epsilon'+\omega}\right)^{\frac{1}{2}}\left[1+\frac{2ad}{c(\epsilon'+\omega)^2}\left(\frac{\epsilon'+\omega}{\omega}\right)^{\frac{1}{2}}\right]^{-\frac{1}{2}}\right\}$$
$$+\frac{6adA}{c(\epsilon'+\omega)^4}\left\{\left[1+\frac{2ad}{c(\epsilon'+\omega)^2}\right]^{-\frac{1}{2}}-\left[1+\frac{2ad}{c(\epsilon'+\omega)^2}\left(\frac{\epsilon'+\omega}{\omega}\right)^{\frac{1}{2}}\right]^{-\frac{1}{2}}\right.$$
$$-\log_e\left[1+\left(1+\frac{2ad}{c(\epsilon'+\omega)^2}\right)^{\frac{1}{2}}\right]$$
$$\left.+\log_e\left[\left(\frac{\omega}{\omega+\epsilon'}\right)^{\frac{1}{2}}+\left(\left(\frac{\omega}{\omega+\epsilon'}\right)^{\frac{1}{2}}+\frac{2ad}{c(\epsilon'+\omega)^2}\right)^{\frac{1}{2}}\right]\right\}. \quad (29)$$

This result is plotted in Fig. 6 normalized to $j(\epsilon')=1$ at the maximum, for $\omega=0.5$ eV and also for $\omega=1$ eV.[13]

[13] The electron affinity for most insulators is not well known. For MgO values, as low as 0.3 eV have been quoted; compare W. G. Shepherd, Wright Air Development Center Technical Report 57-760, Astia Doc. No. AD155852 (unpublished), p. 37. For alkali halides, values of the order of 0.8 eV have been calculated; compare F. Seitz, *The Modern Theory of Solids* (McGraw-Hill Book Company, Inc., New York, 1940), Chap. XI.

The curve is bell-shaped as is always found experimentally; for the data chosen the maximum occurs at 3 eV for $d=100$ Å and 5 eV for $d=300$ Å. The shape of the curve is not too different from the experimental measurements on MgO by Whetten and Laponsky.[14] In Fig. 6 we have plotted $j(\epsilon')/j(\epsilon_{max})$ vs ϵ'/ϵ_{max} (where ϵ_{max} refers to the maximum in the energy distribution) and the data of these experiments for a primary excitation of 800 eV. The fit is reasonably close. However, the following differences should be noted: (1) The position of the maximum observed at 800-eV primary energy is 1.2 eV which is smaller than the value for ϵ_{max} in Fig. 6. Here it should be borne in mind that the parameters c and a given before are only estimated up to the order of magnitude and can easily be adjusted to yield smaller values of ϵ_{max}; (2) experimentally in MgO the position of the maximum is independent of primary excitation energy. The present result does not have this feature, which may be attributed to the assumption of a localized source at x_0. It is to be expected that a "constant loss" theory[10] including a uniform distribution of production sources over a certain depth considerably modifies the result in this respect. Also a much more accurate expression for the source function as dependent on primary energy would be required to explain the primary energy dependence of the curves as observed by Whetten and Laponsky.

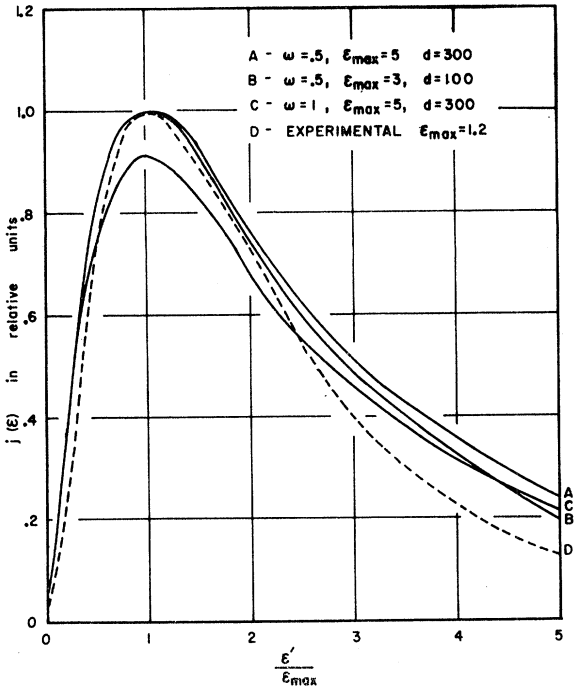

FIG. 6. Energy distribution of external secondaries for various values of electron affinity and range of primaries. Curves A and C are normalized with respect to the maximum for $\omega=0.5$ eV, $d=300$ Å, and for $\omega=1.0$ eV. Curve B is normalized with respect to the maximum for $\omega=0.5$ eV, $d=100$ Å. The dashed curve is the experimental curve obtained by Whetten and Laponsky for 800-eV primary energy.

[14] N. R. Whetten and A. B. Laponsky, Phys. Rev. **107**, 1521 (1957).

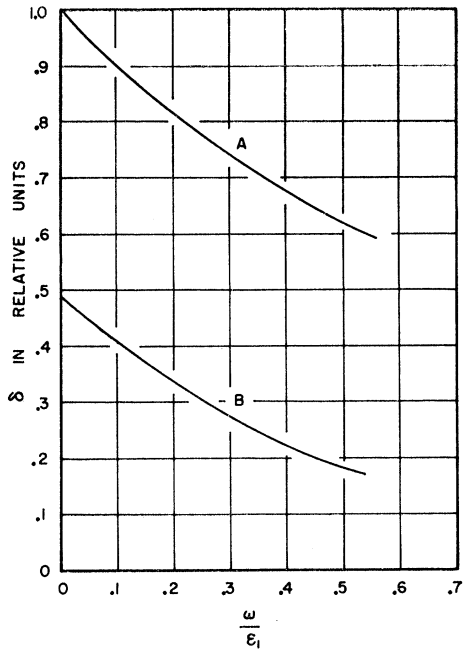

FIG. 7. Variation of total secondary emission coefficient with the electron affinity. Curve A is for $\epsilon_{00}/\epsilon_1=\infty$; curve B is for $\epsilon_{00}/\epsilon_1=1.63$.

D. The Total Secondary Emission Coefficient δ

The total current is found to be from Eq. (19):

$$\delta=\frac{Ac}{3ad}\left\{(\epsilon_1^2+\omega^2)^{\frac{1}{2}}-\left[\left(\frac{\omega}{\epsilon_{00}}\right)^{\frac{3}{2}}\epsilon_1^2+\omega^2\right]^{\frac{1}{2}}\right\}$$
$$-\frac{A}{\epsilon_{00}}\left\{\left(1+\frac{\epsilon_1^2}{\epsilon_{00}^2}\right)^{\frac{1}{2}}-\left[\frac{\omega}{\epsilon_{00}}+\left(\frac{\omega}{\epsilon_{00}}\right)^{\frac{1}{2}}\frac{\epsilon_1^2}{\epsilon_{00}^2}\right]^{\frac{1}{2}}\right\}$$
$$+\frac{A\epsilon_1^2}{\epsilon_{00}^3}\log\frac{1+(1+\epsilon_1^2/\epsilon_{00}^2)^{\frac{1}{2}}}{(\omega/\epsilon_{00})^{\frac{1}{2}}+[(\omega/\epsilon_{00})^{\frac{1}{2}}+\epsilon_1^2/\epsilon_{00}^2]^{\frac{1}{2}}}. \quad (30)$$

Figure 7 gives the relative δ values as a function of ω/ϵ_1 for various values of the parameter ϵ_{00}/ϵ_1 where $\epsilon_1=(2ad/c)^{\frac{1}{2}}$. No measurements on the dependence on electron affinity for insulators are known to date. Such measurements should be carried out on the same material; the electron affinity might be changed by putting suitable overlayers on the crystals, as is presently being undertaken at the University of Minnesota.

6. CONCLUSIONS

The above theory which is based on very simplifying assumptions concerning scattering and the source distribution, nevertheless, shows clearly the difference

with transport in metals in which different excitation and slowing down processes prevail.

The distribution function can be given in closed form with x, ϵ, μ, range d, electron affinity ω, and scattering parameters a and $\lambda(\epsilon)$ as variables.

The resulting energy dependence is roughly in accord with the experimentally observed bell-shaped curves. However, the dependence of the curves on primary energy is not contained in the model. A more sophisticated excitation function is needed.

The energy angular dependence seems to be somewhat deviating from the $\cos\theta'$ law, being elongated to the polar axis for energies of the order of the electron affinity.

The dependence of the total secondary emission coefficient on electron affinity ω is calculated and found to resemble a linear decreasing function for not too high ω.

The present calculations neglect the effect of an electric field which might affect the motion of the secondaries. Calculations, when such a field is present, have now been carried out and will be reported in the future.

ACKNOWLEDGMENTS

We would like to express our appreciation to Dr. A. J. Dekker for suggesting this problem. We also acknowledge the encouragement by Dr. W. G. Shepherd and the facilities provided by him. We have benefited from the group discussions arranged by Dr. W. T. Peria.

APPENDIX

The equation to be solved after the transformations mentioned in the text is

$$\mu\frac{\partial\psi}{\partial x}(x,\eta,\mu)-a\frac{\partial\psi}{\partial\eta}(x,\eta,\mu)=\sigma(x,\eta,\mu), \tag{A1}$$

where we recall

$$\sigma(x,\eta,\mu)=S(x,\eta,\mu)/\lambda(\eta). \tag{A2}$$

We take the Fourier transform with respect to x:

$$\psi(x,\eta,\mu)=\frac{1}{(2\pi)^{\frac{1}{2}}}\int_{-\infty}^{\infty}A(k,\eta,\mu)e^{ikx}dk \tag{A3}$$

$$\sigma(x,\eta,\mu)=\frac{1}{(2\pi)^{\frac{1}{2}}}\int_{-\infty}^{\infty}B(k,\eta,\mu)e^{ikx}dk. \tag{A4}$$

This yields the transformed equation

$$\frac{dA(k,\eta,\mu)}{d\eta}-\frac{i\mu k}{a}A(k,\eta,\mu)=-\frac{1}{a}B(k,\eta,\mu). \tag{A5}$$

Hence,

$$A(k,\eta,\mu)=-\frac{1}{a}e^{i\mu k\eta/a}\int_{\eta}^{\eta_0}B(k,\eta',\mu)e^{-i\mu k\eta'/a}d\eta'. \tag{A6}$$

Here, η_0 is chosen so that $A(k,\eta,\mu)$ and therefore, $\psi(x,\eta,\mu)$ vanishes at η_0.

If the source function $S(x,k,\mu)$ and hence $\sigma(x,\eta,\mu)$ is such that the inversion integral given by (A3) converges uniformly for all η, we can interchange the order of integration over η' and the integration for inversion. Then we get

$$\psi(x,\eta,\mu)=\frac{1}{(2\pi)^{\frac{1}{2}}}\frac{1}{a}\int_{\eta}^{\eta_0}d\eta'\int_{-\infty}^{\infty}B(k,\eta',\mu)\times\exp\left\{ik\left[x+\frac{\mu}{a}(\eta-\eta')\right]\right\}dk. \tag{A7}$$

Recognizing $\sigma(x,\eta,\mu)$ from (A4), we obtain

$$\psi(x,\eta,\mu)=\frac{1}{a}\int_{\eta}^{\eta_0}\sigma\left[x+\frac{\mu}{a}(\eta-\eta'),\eta',\mu\right]d\eta'. \tag{A8}$$